Anais XIV Simpósio Brasileiro de Sensoriamento Remoto, Natal, Brasil, 25-30 abril 2009, INPE, p. 7235-7242.

Multi Application Purpose SAR (MAPSAR) Mission – Ongoing Work During Phase B

José Luis Bueso Bello [1]
Dr. Bjoern A. Dietrich [1]
Fritz Jochim [1]
Dr. Thomas Neff [1]
Dr. Leri Datashvili [2]

[1] German Aerospace Center – DLR
PO-Box 1116, 82230 Wessling, GERMANY
www.dlr.de

[2] Institute of Lightweight Structures – LLB, Technische Universität München
Boltzmannstrasse 15, 85747 Garching, GERMANY
www.llb.mw.tum.de

Abstract. The following paper highlights some interesting aspects, which at the moment are investigated within the phase B study of the MAPSAR mission. The phase A (feasibility) study of the mission was finalized last year and shows all possible critical items, where we deepen our investigation to find cost efficient solutions and/or build up bread-boards to minimize risk. A short overview of the actual status is followed by a presentation of the bread-board of the enfoldable reflector system. Thereafter an insight into the ongoing work of optimizing the orbit and the needed Δv is given.
Keywords: Synthetic Aperture Radar, Earth Observation, Satellite.

1. Introduction

The space-based remote sensing field is changing from one that contains governmental and military systems with high complexity and expense to one that is characterized by hybrid government-commercial systems, fully commercial systems, specific missions based on small satellites, international proliferation, and an increasing emphasis on the production of end-user products. It should be noted that over its history, civilian Earth observation has been dominated by government funded systems.

Missions based on imaging radar have been flying for almost 30 years. The past decade has seen significant growth in research and application, focused on developing approaches for using SAR (**S**ynthetic **A**perture **R**adar) for resources assessment, management and monitoring the environment. German systems like SAR-Lupe and TerraSAR-X are very successful and are able to deliver images of high quality.

At the moment the main focus of German investigation with respect to SAR-technology lies on X-band, which means the frequency band between 8 and 12 GHz. The short wavelength (25 – 37.5 mm) leads to a reflection of the emitted wave nearly at the surface.

Using a longer wavelength like in L-band leads to a deeper intrusion, and additional information can be made available, like humidity of the surface or composition of the terrain beneath forested areas.

In the user community there is a large interest in this kind of information, and this is the reason, why the cooperation between INPE and DLR, lasting for already more than 30 years, was used for starting investigations to perform an L-band SAR mission.

2. Overview of the MAPSAR mission

MAPSAR is a small satellite within the 500 kg class, using the Brazilian Multi Mission Platform (MMP) as satellite bus carrying a SAR sensor. Table 1 shows an extract of sensor specific requirements.

Table 1. Extract of sensor specific requirements.

Frequency	L-band
Polarization	single, dual and quad. pol.
Incidence angle interval	20 - 45 deg
Spatial resolution	3 - 20 meters
Instantaneous swath width	20 - 55 km
Look direction	left/right looking at both ascending/descending path
Additional requirement	Interferometry and Stereoscopy
Noise equivalent σ_0 (NESZ)	-30 dB (quad, dual polarization) -20 dB (single polarization)

The SAR sensor was designed and discussed in all its components: the sensor electronics unit with its radio frequency sub-unit (RFSU) and its processing and control sub-unit (PCSU), the amplification and power combining concept, the antenna feed horn and antenna reflector system, as well as a custom waveguide design and a complete accommodation into the payload module carrier.

The most innovative components might be the power concept, see Figure 1, and the antenna design. The actual investigations with respect to the antenna are given in Chapter 4.

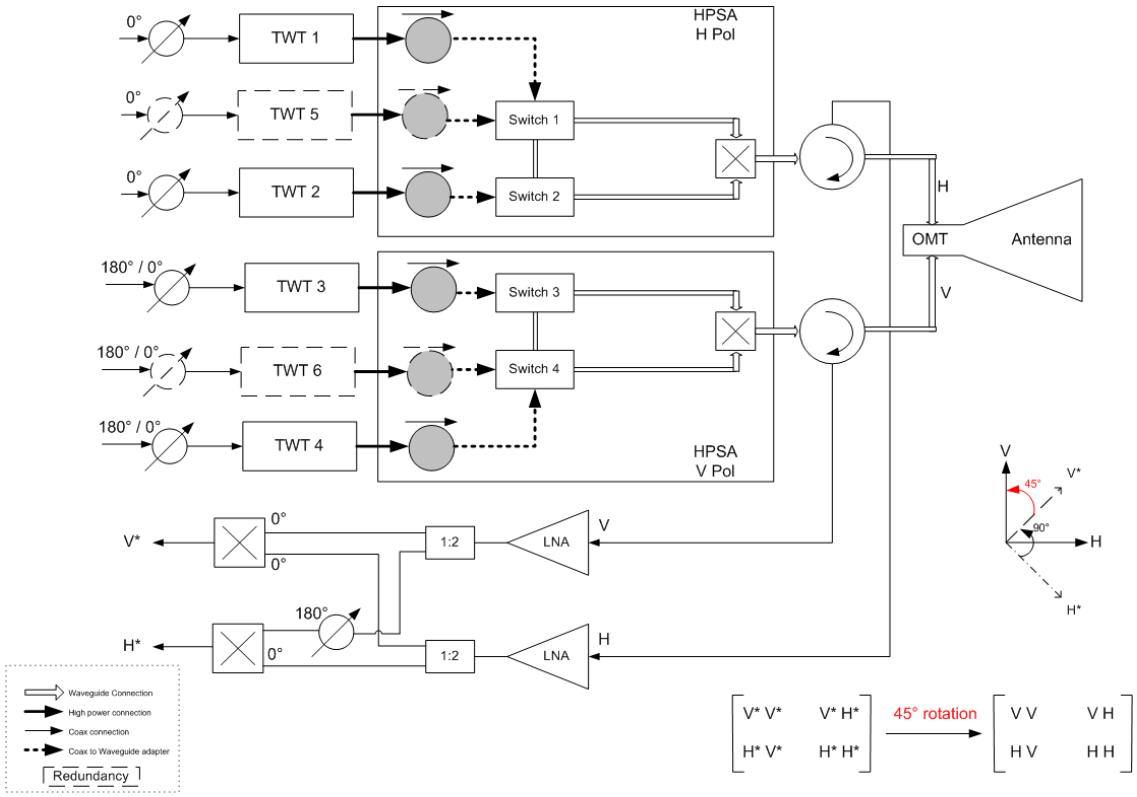

Figure 1. Power combining concept with polarization synthesis. TWT: traveling wave tube; H Pol: horizontal polarization; V Pol: vertical polarization; OMT: ortho mode transducer

Based on the user requirements, MAPSAR offers three different resolution modes (down to 3 m, 10 m and 20 m) operated in the conventional stripmap mode. The chirp bandwidth is designed to use the full 85 MHz allowed by the World Administrative Radio Conference.

This leads to a high resolution mode up to 3 m. For lower resolution modes the bandwidth is reduced accordingly. The quad polarization mode is foreseen for the low resolution, and the single polarization is foreseen for the high resolution to ensure sufficient sensitivity. The medium resolution can be operated in dual or single polarization modes, see also Table 2 and Figure 2.

Table 2. MAPSAR modes with performance parameters

	incidence angle in deg	swath width in km		spatial resolution in m	
		near	far	near	far
HR: high resolution / single pol.	20 - 48	38	20	4	3
MR: medium resolution / dual pol.	20 - 49	43	43	10	10
LR: low resolution / full pol.	20 - 36	40	24	20	20

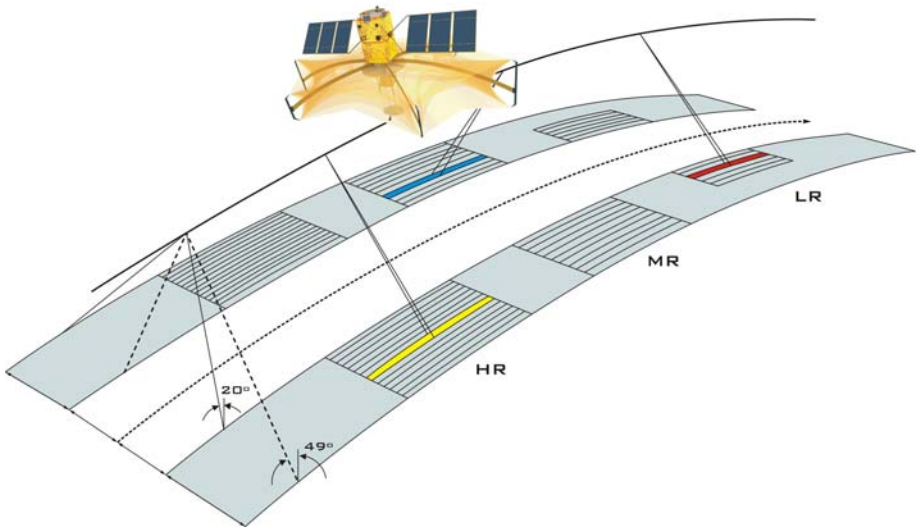

Figure 2. Illustration of the MAPSAR geometry in three different modes

The satellite is capable of acquiring SAR data in both left and right looking geometry. The whole satellite will be rotated to have access to the region of interest. In this way, incidence angles between 20 and 45 deg can be operated and the minimum swath width will be larger than the required 20 km. The sensitivity in terms of the noise equivalent sigma zero (NESZ) is better than -30 dB in the fully polarimetric mode. The sensor will reach a PSLR better than 24 dB and the ambiguity suppression is usually better than -18 dB. In summary, the sensor performance is compliant with most of the user requirements and will guarantee excellent image products. In addition, stereoscopy and interferometry shall be possible with MAPSAR, which is highly dependent on the orbit. The actual investigations with respect to the orbit are mentioned in chapter 5.

3. Programmatics

The phase A (feasibility) study of MAPSAR was finalized end of 2006. At the moment we are working on the phase B (detailed analysis), which will last until end of 2009. The launch of the MAPSAR spacecraft is scheduled for 2013.

One major milestone of the phase B study is to build up a bread-board of the enfoldable antenna system, which is described in detail in Chapter 4.

4. Antenna bread-board

4.1 Antenna requirements

The selected antenna configuration for MAPSAR is a Cassegrain reflector antenna, see Figure 3, with a main reflector of 7.5 m in azimuth and 5 m in elevation, a hyperbolic sub-reflector, both with an elliptical rim, and an L-band horn feed.

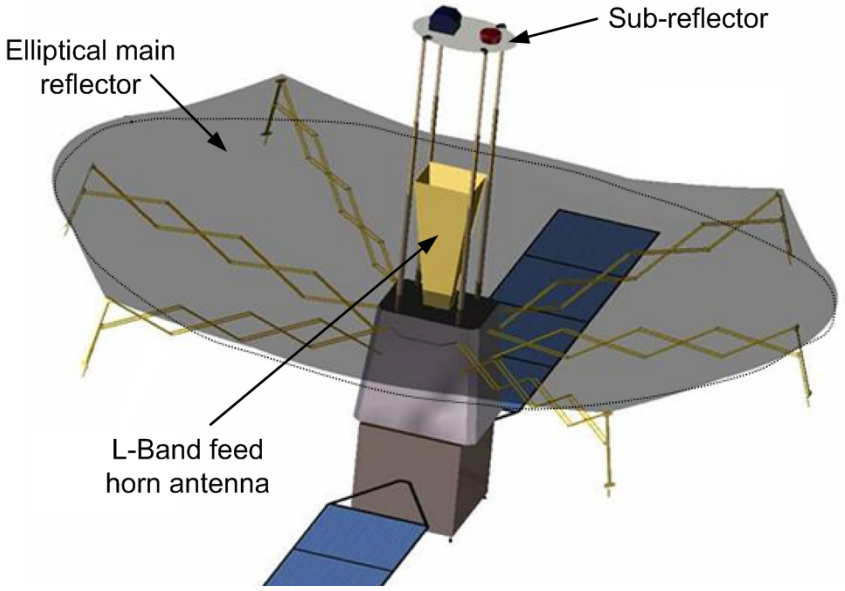

Figure 3. MAPSAR satellite with its cassegrain reflector antenna

Due to the large reflecting surface and the weight limitations imposed by the MMP platform, a lightweight material for the main reflector is needed. The shell membrane antenna reflector technology (SMART) concept developed at the LLB was selected for the construction of the reflector, Baier et al. (2006), with a non-tensioned reflecting surface and a deployable backside structure consisting of hybrid foldable membranes.

Different antenna requirements were established: Tables 3 and 4 present the surface accuracy and RF requirements imposed to the antenna materials.

Table 3. MAPSAR surface accuracy antenna requirements

RMS	Gain degradation	Medium sidelobe isolation	Strong sidelobe requirement
L-Band (λ = 24 cm)	< λ/50 = 4.8 mm	< λ/100 = 2.4 mm	< λ/300 = 0.8 mm

Table 4. MAPSAR RF antenna requirements

	Reflection loss	Depolarization	Amplitude variation	Phase variations	Transmission coefficient
RF performance	< 0.1 dB	< -40 dB	< 0.02 dB	< 2 deg	< -20 dB

Additional mechanical requirements comprise the deployment mechanisms (antenna stiffness requirements for deployed and stowed configurations) and the reflector weight, which will not exceed 70 kg.

These requirements have to be satisfied by the selected antenna. During the phase B, a scaled engineering model antenna has been built to prove the reliability of the employed concept, materials and technologies. In the following, the model and the results of the different tests are presented and discussed.

4.2 MAPSAR antenna reflector structure and bread-board model

The MAPSAR structure consists of six scalable radial main ribs (radially deployable pantographs with profiled membranes), attached to the solid central unit. In between the radial ribs, a system of auxiliary membrane ribs supports the reflecting surface and ensures the sufficient stiffness for the antenna. The auxiliary ribs are connected to pantographs using spring adapters. Figure 4 shows this configuration.

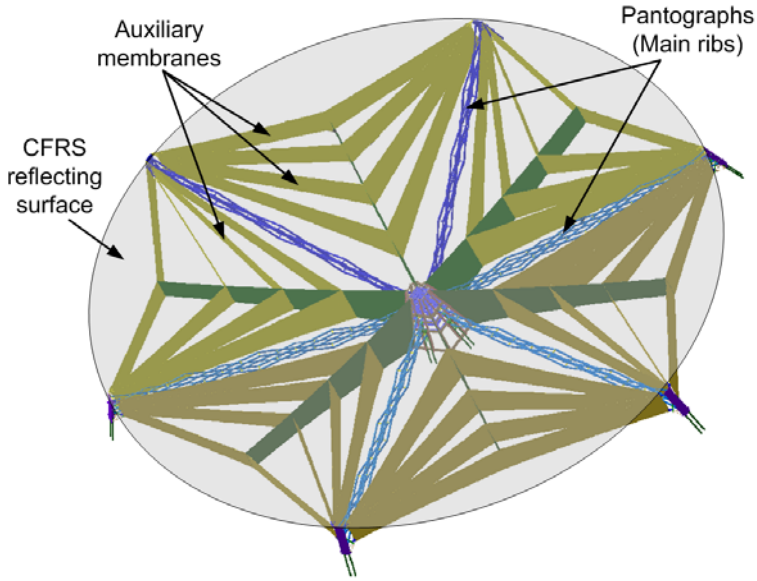

Figure 4. MAPSAR structural concept (main ribs showed without profiled membranes)

Triax carbon fibre reinforced silicone composite (triax CFRS) is used as material for the membrane ribs and the reflecting surface, Datashvili (2008). The carbon fibre fabric provides reflectivity and dimensional stability of the surface while silicone is responsible for flexibility and some finite bending stiffness of the composite. This material permits easy stowing and deployment of all membranes, and its flexibility ensures a high accurate double-curved reflecting surface.

A scaled model with an aperture diameter of 1.6 m has been built to verify and qualify all structural and technological procedures used to build the reflector. Figure 5 shows three stages of the performed deployment test. During the deployment, pantographs are extended radially by an electric motor.

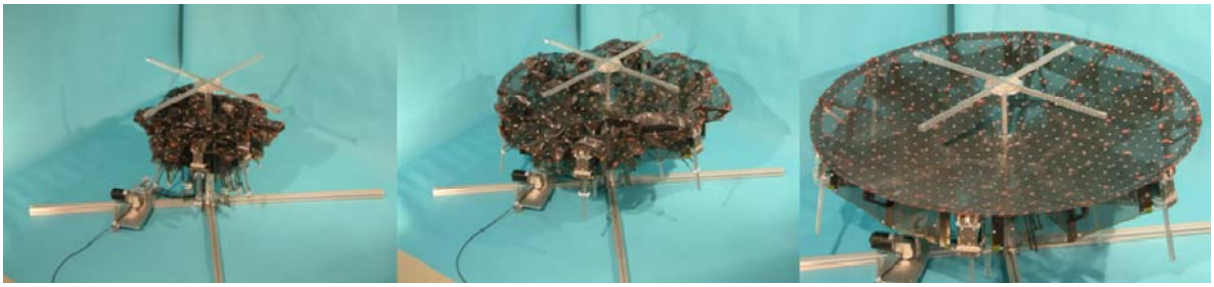

Figure 5. Bread-board antenna deployment procedure

This bread-board antenna model enables to carry out a number of different tests for verification of the conceptual design ideas and analysis tools developed. It will also be used to identify possible weak points and to verify the reliability of the deployment mechanism, Datashvili and Baier (2008).

4.3 MAPSAR antenna analysis and tests

In the deployment mechanism test, see Figure 5, the high reliability and synchronization of the deployment mechanism were fully confirmed. A previous demonstrator with an umbrella deployment mechanism was manufactured to prove the root-mean-square (RMS) surface accuracy of the triax CFRS material. This demonstrator was undertaken a series of deployment tests under earth gravitation-compensated conditions within parabolic flights, and with precision photogrammetry techniques under different laboratory conditions at LLB facilities, Datashvili et al. (2006). In all calculations the total RMS accuracy budget including all sources of deviations did not exceed 0.5 mm, which is in concordance with the MAPSAR surface accuracy antenna requirements, see Table 3.

RF characterization tests were performed in three different measurement facilities and the results show the possibilities of using the CFRS material as reflecting surface for frequencies even higher than the required L-band. Table 5 summarizes the obtained measurement results in the RF range from 5.5 GHz to 8 GHz, which fully satisfied the RF antenna requirements shown in Table 4 for L-band.

Table 5. MAPSAR RF antenna measurement results

	Reflection loss	Depolarization	Amplitude variation	Phase variations	Transmission coefficient
RF performance	< 0.13 dB	< -42 dB	< 0.02 dB	< 0.5 deg	< -21 dB

The characterized lightweight material allows the MAPSAR reflector antenna to fulfill the mission requirements in terms of mass and stowed volume as well. Simulations demonstrate that also the eigenfrequency conditions in stowed and deployed configuration are fulfilled.

Finally, using a fully parametric finite element model, thermo-mechanical analyses were performed. All these analyses demonstrate that the selected structure and the characterized materials for the MAPSAR antenna can be successfully used for space applications.

5. Orbit design and orbit keeping

During phase A of the MAPSAR study, two different Sun-synchronous orbits were investigated in order to cover all user requirements: repeat pass SAR interferometry as well as SAR stereoscopy. In the present study an alternative orbit concept will be investigated: combining the MAPSAR orbit with the TerraSAR-X (TSX) orbit to allow complementary observations. The reproducible interferometric orbit shall be the primary requirement, whereas SAR stereoscopy should be possible in addition. In the present study, a non Sun-synchronity is accepted in order to keep the orbit reproducibility.

5.1 Reference orbit assumption

The TerraSAR-X orbit is Sun-synchronous with ground a track reproducibility after 11 days and 167 draconic periods. The corresponding mean Keplerian orbital elements are: semimajor axis a = 6892.9 km (equivalent to mean equatorial height H = 514.8 km), circular, inclination i = 97.44 deg, ascending node at 18:00 mean local time (dust orbit). For MAPSAR the present study assumes a circular orbit with inclination i = 100 deg. The orbital height has to be derived from the condition of the multipass interferometry as near as possible to the TerraSAR-X orbit.

5.2 Orbit selection considerations

In order to allow multipass SAR interferometry, the effective baseline B_{eff}, compare Figure 6, will be used as characteristic parameter. The interferometric observation will be undertaken from the two satellite positions S_1 and S_2. These positions are separated by the central angle difference $\Delta\gamma$. A mathematical relation between the effective baseline and the central angle difference can be derived using Figure 6.

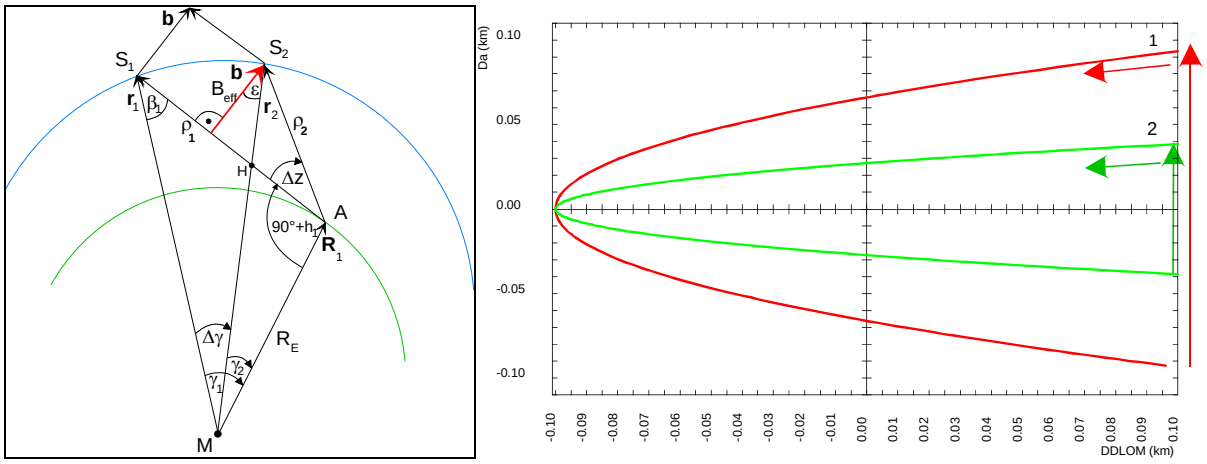

Figure 6, left: The computation of the effective baseline for multipass SAR interferometry between the two satellite positions S_1 und S_2, under the assumption of a circular satellite orbit and related to a spherical primary body. right: Orbit correction cycle (correction in semimajor axis) for H = 535 km MAPSAR orbit (reproducibility about 11:164) for node crossing accuracy ±100 m, for solar maximum (curve 1) and solar minimum (curve 2)

For an L-band SAR sensor, an average value of $B_{eff} \approx 0.7$ - 1.0 km for the effective baseline will be taken into account. Assuming the orbital height H = 515 km and the average incidence angle of 28 deg, the corresponding central angle difference will be about $\Delta\gamma = 0.01$ deg.

In order to respect such a small amount with respect to a given reproducibility of a reference orbit, a suitable subcycle has to be found. This subcycle of an alternative orbit has to be controlled with the request of fulfilling the interferometric condition. Assume K periods of the node for track reproducibility of a reference orbit within N draconic periods, as well as an additional shift $\Delta\gamma$ of the satellite position allowing an interferometric observation. Then the mean shift of nodal longitude per one draconic period for the new orbit will be calculated using Equation (1).

$$\overline{\Delta\lambda_{\Omega}} = -\left(K \cdot 360° + \Delta\gamma\right) / N \qquad (1)$$

This value including the mean inclination and eccentricity of the desired orbit allows the calculation of the mean semimajor axis of the new orbit. This new orbit is extremely related to the selected inclination. In order to keep the K = 11 days reproducibility of the node and in order to be higher than the TSX orbit for an orbit with inclination i = 100 deg, N = 166 will be selected for the number of draconic periods. An orbit with semimajor axis a = 6915.552 km will be obtained (averaged orbital height at equator H = 537.4 km).

Table 6 lists the fuel amount for a satellite lifetime of 4 years together with other detailed information to get a feeling which fuel amount has to be taken into account for orbit keeping for a (more or less) stable interferometric orbit. Based on the assumptions of a satellite launch

mass $m_0 = 530$ kg, an average satellite area of 8 m^2, the air drag coefficient $c_D = 2.2$, the use of a hot gas engine (exhaust velocity $c_e = 2.8$ km/s, rocket motor factor $R_C = 0.85$) for the correction maneuvers, the velocity increment Δv and the corresponding fuel need will be calculated for the whole lifetime. In the example of Figure 6 the correction cycle with respect to a tolerance interval of the nodal crossing of ±100 m is presented. The corresponding data is also given in Table 6. As well known, the total fuel need is independent of the number and duration of the single correction cycle intervals. Therefore, the last data in Table 6 is representative in any case. In the case of the MAPSAR interferometric orbit, a repeatable correction cycle with respect to the repetition cycle K should be achieved. Only by this way a reproducible satellite position for interferometric observation can be envisaged.

Table 6. Velocity increment and fuel need for a 4 years lifetime for orbit keeping with respect to air drag influence.

	Air density ρ	Orbit decay	Variation in semimajor axis per cycle Δa	Velocity increment per cycle ΔV_{cycle}
Solar maximum	1.267 g/km^3	$-0.2209 \cdot 10^{-5}$ km/s	±0.093 km	0.102 m/s
Solar minimum	0.2042 g/km^3	$-0.3722 \cdot 10^{-6}$ km/s	±0.038 km	0.042 m/s
	Fuel need per cycle Δm	Cycle time T_{cycle}	Along track error per cycle ΔL	Total Velocity increment ΔV
Solar maximum	0.019 kg	1.0 days	±3.3 km	153.835 m/s
Solar minimum	0.008 kg	2.4 days	±3.3 km	25.790 m/s
	Total fuel need Δm		Possible payload mass	
Solar maximum	28.333 kg		496.7 kg	
Solar minimum	4.859 kg		524.3 kg	

6. References

Arbinger, Ch.; d'Amico, S.: Impact of Orbit Prediction Accuracy on Low Earth Remote Sensing Flight Dynamics Operations, **ISSFD_XVIII34,** 2004.

Baier, H.; Datashvili, L.; Nathrath, N.: The deployable precision shell-membrane reflector SMART, Proc. Euro. Conf. on Antennas and Propagation, **Eucap 2006**, Nice, France, Nov. 2006.

Datashvili, L.; Lang, M.; Huber, M.; Baier, H.: Accuracy study of a space deployable antenna reflecting surface under 0g and 1g conditions. **Deutscher Luft- und Raumfahrtkongress 2006**, Braunschweig, Deutschland, published in the proceedings of 2007, band III-IV.

Datashvili, L.: Multifunctional Dimensionally Stable Flexible Composite for Space Applications, Proceedings of **59th International Astronautical Congress 2008**, Sep. 2008, Glasgow, Scotland.

Datashvili, L.; Baier, H.: Precision Deployable Shell-Membrane Antenna Reflector for Space Applications, Proceedings of **59th International Astronautical Congress 2008**, Sep. 2008, Glasgow, Scotland.